Conductance Fluctuations in Chains of Particles Arising from Conformational Changes of Stabilizer Molecules

L. V. Govor and J. Parisi

Institute of Physics, Carl von Ossietzky University of Oldenburg, D-26111 Oldenburg, Germany

Reprint requests to L. V. G.; E-mail: leonid.govor@uni-oldenburg.de

Z. Naturforsch. **68a,** 157 – 164 (2013) / DOI: 10.5560/ZNA.2012-0076
Received July 31, 2012 / published online February 15, 2013

Dedicated to Alfred Klemm on the occasion of his 100th birthday 15 February 2013

We have bridged a pair of gold electrodes with various arrangements of gold nanoparticles stabilized with citrate molecules. The resulting devices exhibited current fluctuations at a constant bias voltage and fluctuations of the differential conductance as a function of the bias voltage. These fluctuations were attributed to the interplay of molecular conformation, charge switching, and breaking of the links at the interface molecules–electrode. We found that, for all investigated samples, the contact resistance at the interface molecules–electrode was by about one order of magnitude larger than that between nanoparticles coupled by citrate molecules. We conclude that the mechanism of charge transport can be viewed as a series of discrete steps involving initial hopping (injection) of the charge from the left-hand-side gold electrode to the molecules, tunnelling of the charge through the molecules–nanoparticle–molecules (MNM) unit, hopping to the next MNM unit, etc., and finally hopping (extraction) of the charge to the right-hand-side gold electrode.

Key words: Nanoparticle; Citrate Molecules; Charge Transport; Conductance Fluctuations.

1. Introduction

Charge transport through nanoparticle (NP) assemblies represents a fundamental process that controls their physical properties, which are determined by the coupling and arrangement of individual NPs and depend on their size, shape, and composition. Theory and experiments unveil that, at sufficiently low temperature below a threshold voltage V_t, no current flows through the particle array, while above V_t the current increases, according to the power law $I \sim (V - V_t)^{\zeta}$ with $\zeta = 1$ in a one-dimensional and ranging between $5/3$ and 2 in a two-dimensional array [1 – 3]. I denotes the current, V the voltage. Electronic coupling between individual particles is influenced by inter-NP spacing and by stabilizer molecules capping the NPs. The inherent possibility of a switching between different molecular conformations represents one peculiarity of these molecules which can strongly influence charge transport. Citrate represents a common electrostatically stabilizing agent for gold NPs, because the particles are typically synthesized through a citric acid reduction reaction [4]. Switching of the molecular conductance of citrate was demonstrated by Wang et al. [5], where they used mechanical stretching of two conformers of citrate capped on and linked between the gold NPs.

The influence of stabilizer molecules on charge transport through NP arrays has been reported recently [6 – 8], where we have examined charge transport between two gold electrodes bridged by a single gold NP or by one- and two-dimensional chains of those (about 8 – 10 particles within the chain). Such a configuration exhibits linear current–voltage (I–V) characteristics and current fluctuations in the range 3 – 100 mHz at constant bias voltage. Moreover, we observed fluctuations of the differential conductance as a function of the bias voltage. We assume that these fluctuations arose from equally probable conformational changes of all citrate molecules along the chain of NPs induced by charge transfer through those, independently of their location along the chain of NPs or at the electrode interface. In following, we present a comparative analysis of I–V characteristics for chains of NPs having variable size (both length and width). We demonstrate that the resistance between gold electrodes and gold NPs coated with citrate molecules is significantly higher as compared to the resistance between two such citrate-coated NPs. The conduc-

tance fluctuations can be attributed to interplay between the molecular conformation, charge switching, and breaking of the bonds, taking place at the interface molecule–electrode. We found that the main contribution to the charge transport in chains of NPs resulted from hopping.

2. Experiment

Figure 1a schematically illustrates the configuration investigated. The initial Au/Cr contact pads located on a SiO_2/Si substrate were formed by photolithography, where gold and chromium thin films have been electron beam deposited. The layer sequence (and thickness) from top to bottom is Au (20 nm)/Cr (5 nm)/SiO_2 (230 nm)/Si (0.7 mm). A 100 nm or 200 nm wide, 32 nm deep, and 4 μm long nanogap between electrodes has been formed by focused ion beam (FIB) patterning [9]. Hereto, we have used a dual beam system (FEI Helios Nanolab 600), combining a 30 keV (1 pA) gallium ion beam with a scanning electron microscope (SEM). After FIB patterning, we measured a resistance of the non-connected gold electrodes of each sample being larger than $10^{14}\,\Omega$ (Keithley 6430). The samples and the corresponding two-pin holder were placed into a double-shielding box for measurement.

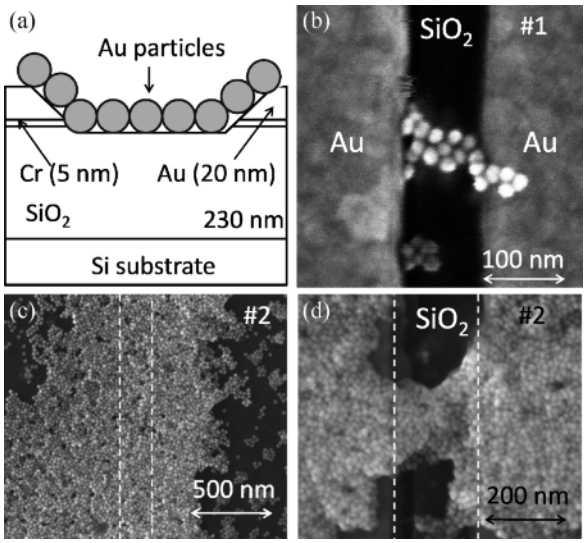

Fig. 1. (a) Schematic illustration of the NP chain located in between two gold electrodes. (b) SEM image of the small chain of particles (Sample 1) connecting the gold electrodes. (c) and (d): SEM images of the wide chain of particles (Sample 2) connecting the gold electrodes before and after FIB patterning, respectively. The dashed lines indicate a gap between the gold electrodes.

Deposition of NPs in between the gold electrodes was achieved via pinning the droplet edge of the solution with a concentration of $1.2 \cdot 10^{11}$ particles/mL at the appropriate position between the gold electrodes [9, 10]. As a result, a concentric ring-like array of NPs forms along the droplet edge. The size of the array strongly depends on pinning time and substrate temperature. After having positioned the NPs in between the gold electrodes, the place surrounding a desired particle chain was additionally patterned with FIB. With this procedure, unwanted connections between the electrodes were removed. As examples, two representative samples are shown in Figure 1b – 1d, where the gold electrodes are bridged by a different number of gold particles.

3. Experimental Results

The I–V characteristics of the samples investigated were recorded by two-contact-mode measurements at 300 K. A maximal bias voltage V applied to each sample was taken in correspondence to the resistance of the sample. As a criterion in the entire regime of the applied voltage, we have chosen the current so that its maximal value amounted to about 1 pA for small samples and 10 pA for wide samples. It is essential to limit the charge transport, because larger values of the current typically cause degradation of the junction, probably due to excessive heat dissipation or due to local displacement of particles within a chain. We have observed current fluctuations at constant bias voltage. To examine the nature of such peculiarity, we have recorded the current over time at intervals of 625 ms. All five samples investigated show similar and reproducible results. The typical temporal behaviour of the current $I(t)$ at $V = 4$ mV for Sample 1 and at $V = 200$ mV for Sample 2 is displayed in Figure 2a and 2b, where the current randomly fluctuates around a mean value. Figure 2c and 2d illustrate the corresponding distributions of $I(t)$ for Samples 1 and 2, respectively. For a description of the I–V characteristics, we determined a mean value of this distribution, I_0, and its standard deviation, I_s, which we interpreted as fluctuation amplitude. The designation of I_0 and I_s is illustrated schematically in Figure 2. For comparison, we investigated the $I(t)$ behaviour of a resistor

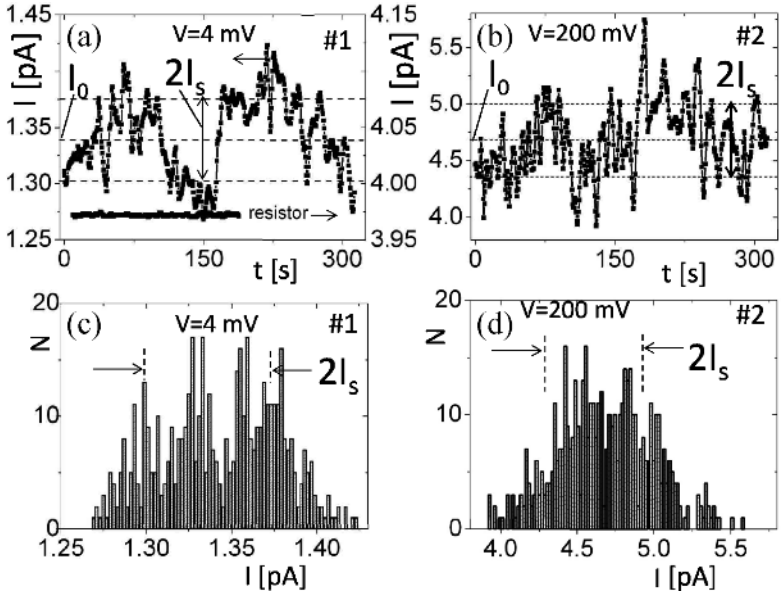

Fig. 2. (a) and (b): Typical time dependence of the current $I(t)$ for Samples 1 and 2 recorded at bias voltage 4 mV and 200 mV, respectively. I_0 and I_s are the mean current and its standard deviation (fluctuation amplitude), respectively. The lower curve in (a) displays the dependence $I(t)$ for a resistor. Note, the I axis span amounts 0.2 pA in (a) and 2 pA in (b). (c) and (d): Corresponding distributions for Samples 1 and 2, respectively.

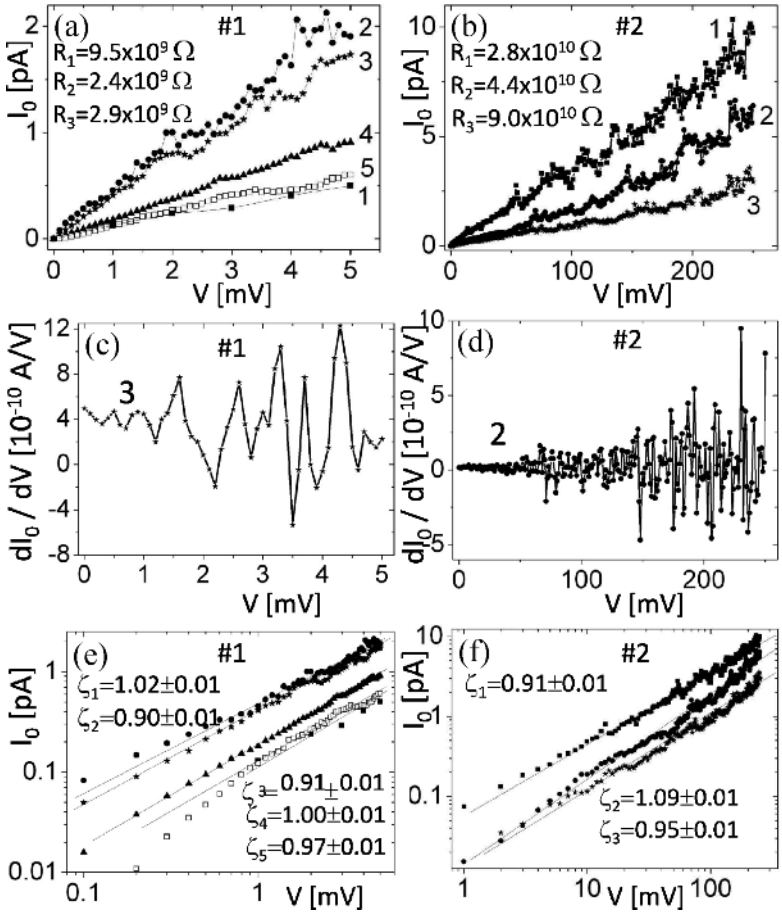

Fig. 3. (a) and (b): I_0–V characteristics measured one after another for Samples 1 and 2. R_1, R_2, and etc. indicate the corresponding values of the sample resistance. (c) and (d): Differential conductance $\mathrm{d}I_0/\mathrm{d}V$ for Sample 1 (Curve 3) and for Sample 2 (Curve 2) shown in parts (a) and (b), respectively. (e) and (f): Log–log plot of the I_0–V curves for Samples 1 and 2 shown in parts (a) and (b) with the best-fit of exponent ζ.

with $1.3{\cdot}10^{10}\,\Omega$ (thermal noise) and did not observe any similarly pronounced fluctuations (lower curve in Fig. 2a). This clearly demonstrates that the fluctuations solely result from the presence of NP junctions. We found that, independent of the configuration of the particle chain, by increasing the current through an increase of the bias voltage, the relative fluctuation amplitude I_s/I_0 amounts to about 0.05, roughly independent of the applied voltage. A Fourier analysis of the $I(t)$ fluctuations measured at different bias voltage indicates that the frequency of the dominant fluctuations lies in the range 3 – 100 mHz [6, 7].

Typical I_0–V characteristics for two samples with a different number of particles in the chain are illustrated in Figure 3a and 3b, respectively. There are two important observations: (i) Two sequentially measured I_0–V curves can exhibit increased conductance of the chain (Fig. 3a). (ii) Subsequently measured I_0–V curves may also have a lower conductance (Fig. 3b). These peculiarities of the individual I_0–V curves can be clearly seen in Figure 3c and 3d, where the dependence of the differential conductance ($\mathrm{d}I_0/\mathrm{d}V$) on voltage is presented. A further important observation is the following: The amplitude of the random fluctuations of the differential conductance increases with the voltage applied. These experimental findings indicate that not only the value of the applied voltage, but also the state of the conducting path in the particle chain, which may depend on the history of the sample, can affect its conductance. Figure 3e and 3f demonstrate that all I_0–V curves shown in Figure 3a and 3b follow the same power-law scaling $I_0 \sim V^{\zeta}$ with an exponent $\zeta \approx 1$. Such value of the exponent ζ indicates a linear behaviour for charge transport in the chain of particles, i.e., a linear conduction path. Again, comparison of the I_0–V curves for a small chain of particles and for a wide chain demonstrates the similarity in behaviour.

4. Discussion

The theoretical approach $I \sim (V - V_t)^{\zeta}$ for the single electron charging effect in arrays of particles developed by Middleton and Wingreen [1] considers only the zero-temperature limit, where the local energy levels are delineated and barriers between neighbouring sites are well defined. That means that, for a bias voltage lower than V_t, charge transport should not occur. The latter differs from the results of our experiment, where due to thermal energy a finite conductance $g_0 = \mathrm{d}I_0/\mathrm{d}V$ even at $V = 0$ and $T = 300$ K takes place. Figure 3c and 3d illustrate that the conductance g_0 amounts to about $5 \cdot 10^{-10}$ A/V and $2 \cdot 10^{-11}$ A/V for Samples 1 and 2, respectively. The linear suppression of the threshold voltage $V_t(T)$ with temperature was considered by Bezryadin et al. [11] and Elteto et al. [12] in studies of one-dimensional nanoparticle chains, where the dependence $V_t(T) \approx V_t(0) - N_p k_B T/e$ was established, where N_p is the number of particles in the chain. That means that, with increasing temperature, the nonlinear I–V characteristics, described by the power law $I \sim (V - V_t)^{\zeta}$, monotonously shifts to the left until a constant conductance g_0 at $V = 0$ is reached. In other words, if energy levels for the transport of electrons from one site to another are distributed within bk_BT, thermally excited electrons can be transferred to neighbouring sites. The parameter b describes the extent of thermal broadening and depends on details of the electronic level distribution ($b = 2.4$, [12]).

Figure 4a schematically illustrates a single particle Au_n with chemisorbed citrate molecules connecting a gold electrode Au_e (on the right). A variety of interactions between citrate molecule and gold electrode is possible, ranging from a physisorption to a chemisorption. The physisorbed citrate molecule interacts only weakly with gold atoms and, correspondingly, charge transfer is more difficult (weak coupling). Chemisorption is characterized by cova-

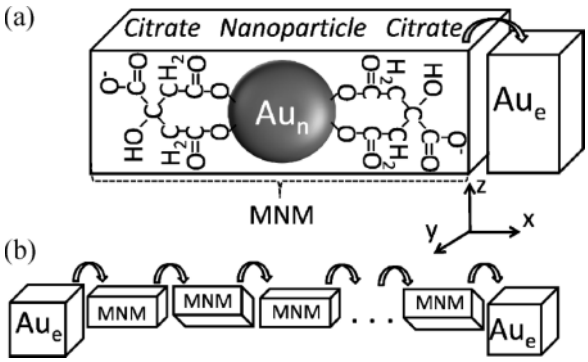

Fig. 4. (a) Schematic illustration of a single gold particle Au_n stabilized with citrate molecules (denoted as MNM, box) connecting a gold electrode Au_e (on the right). (b) Schematic illustration of the one-dimensional chain of particles and hopping transport through that. The rectangular boxes represent MNM units (local hopping site) shown in part (a). The arrows represent thermally activated charge hopping over the barriers between local sites.

lent bonds which makes charge transfer between gold atoms and citrate molecule easier (strong coupling). In between weak and strong coupling, other types of interaction are possible, based on interface effects like integer charge transfer through tunnelling (physisorption), rearrangement of electron densities and attraction through image forces (physisorption), and partial charge transfer (weak chemisorption) [13 – 15]. As a result of metal–molecule coupling, the electron orbitals of citrate molecules can hybridize with states of the gold atoms. Consequently, the original molecular levels broaden and shift compared to a free molecule in vacuum. For example, in the case of covalently linked molecules (chemisorption), the broadening can be several hundred meV [16], i.e., much larger than the thermal energy at room temperature (26 meV).

It was already demonstrated that the maximum saturation coverage of a gold particle by citrate molecules amounts to about 2.7 molecules/nm^2 [17, 18]. For a particle with a diameter of 20 nm, we assume that on average at each Au_e–Au_n junction about 10 citrate molecules oriented in parallel can link the NP to the electrode, and about 20 molecules can transfer a charge across a Au_n–Au_n junction (10 molecules from each particle). Considering the preparation procedure of the devices investigated, we conclude that the citrate molecules are chemisorbed on the gold nanoparticle (bond Au_n–O) and physisorbed on the gold electrode (bond Au_e–O). In other words, in devices where a chain of particles bridges the gold electrodes, the physical links of Au_e–O at the two electrode interfaces determine the properties of the device. That means that the experimentally observed I–V curves are to a large extent determined by the physical bonds Au_e–O, rather than by intrinsic molecular properties or the chemical bonds Au_n–O. The resistance of the devices investigated lies in the range $(10^9 - 10^{11})\,\Omega$, and we conclude that the high device resistance is due to the contact resistance between electrode and molecules. This can be confirmed by comparing the resistance of Sample 1 to that of Sample 2. For geometrical reasons, it was expected that the resistance of Sample 2 will be significantly smaller compared to Sample 1, but it is the wrong way.

For understanding the current fluctuations at the fixed voltage, we take into account (Fig. 2) a molecular switching mechanism that includes conformational changes, electrostatic charge trapping at defects, and metal–molecule contact breaking. The conformational change is consistent with a voltage-induced chemical structure variation involving changes in molecular conformation with charge redistribution along the molecule [19 – 21]. The charge switching can appear when the lifetime of the tunnelling electron on the molecule is sufficiently long by a mechanism that stabilizes the extra charge on the molecule [22 – 24]. The metal–molecule contact breaking is caused by changes in the bond between the molecules and the gold electrode [20]. We assume the following scenario for switching events that may occur at the molecule–electrode interface. By injecting electrons into the citrate molecule, a conformational/orientational change in the molecule is initiated, where the O–C–O group physically connecting to the gold electrode can be rotated around the C–C axis of the citrate molecule [25]. Note, depending on the bias voltage applied to the samples, the thermal energy $k_B T \approx 26$ meV can play an important or even dominant role in the rotation of the O–C–O group. Due to the rotation of the O–C–O group, the length of the distance between electrode and molecule increases. The larger distance reduces the tunnelling coupling between molecule and electrode, and the corresponding ionic reorganization on the surface of the gold electrode due to an added electron on the molecule can even stabilize this charge state. The bare Au_e–O bond energy has been estimated to 90 meV for –COOH adsorption on the gold surface [26, 27], which is too large for allowing the breaking of the bonds at room temperature by an applied bias voltage of few mV only. Thus, the comparatively small activation energy for the breaking of the bonds in the case of our experiments seems to be a consequence of the weakened Au_e–O bonds due to conformational changes of the citrate molecule [20]. In this case, the transmission probability T_e is exponentially sensitive to changes in the distance of the Au_e–O bond, d_e: $T_e \approx \exp(-2kd_e)$, where k is the decay constant. A similar processes can arise at the molecule–molecule interface, where the length of the O–O bond between two molecules connecting neighbouring particles in the junction Au_n–Au_n may be modified during the charge transfer.

Figure 3e and 3f demonstrate that I_0–V curves indicate a linear behaviour for charge transport through the small and the wide chains of particles. Several mechanisms of charge transport through the junctions metal–molecule–metal give rise to the linear I–V characteristics at low bias voltage, which are coherent tun-

nelling, incoherent tunnelling, and hopping. Coherent tunnelling is characterized by the probability of an electron transfer through a barrier of some thickness and height, where the phase of the electron does not change. The transmission rate of the coherent tunnelling decreases exponentially with barrier thickness and is small over distances larger than 2.5 nm, where charge transport can usually be described by an incoherent tunnelling or hopping [28]. In the case of incoherent tunnelling, the electron tunnels along a series of sites separated by potential wells, where the residence time of the electron is large enough to disturb its phase, and the process is formulated as a series of discrete steps. Both, coherent and incoherent tunnelling exhibit two main features: (i) exponential dependence on barrier thickness L and (ii) weak dependence on temperature. These properties are expressed as [29]

$$R = R_0 \exp(\beta L)\,, \tag{1}$$

where R_0 gives the effective contact resistance and $\beta = 2(2m\phi)^{1/2}/\hbar$ a structure-dependent tunnelling attenuation factor. ϕ means the effective tunnelling barrier height, m the electron effective mass, and $\hbar$ Planck's constant.

Hopping is a thermally activated process, where the transmission rate of the electrons follows a classical Arrhenius relation. Hereto, the electron can traverse one or more sites, like in incoherent tunnelling, but for the case of hopping, the involvement of a nuclear motion (bond rotation, bond stretching) becomes necessary. That means, electron transfer over the barrier cannot occur until the thermal motion of nuclei results in a favourable molecular geometry, i.e., the molecule must rearrange for electron transfer. Hopping transport exhibits two main characteristics: (i) the transmission rate varies with barrier thickness as $1/L$, because hopping involves a series of transitions between sites, and (ii) strong dependence on temperature. These properties can be expressed in terms of a resistance as [29]

$$R = R_0 + \alpha L = R_0 + \alpha_\infty L \exp\left(\frac{E_a}{k_\mathrm{B}T}\right), \tag{2}$$

where $\alpha = \alpha_\infty \exp(E_a/k_\mathrm{B}T)$ is a molecular specific parameter with units of resistance per unit length and E_a the activation energy associated with hopping (bond rotation, bond stretching).

For simplicity, we denoted a unit 'molecules–nanoparticle–molecules' as MNM unit (box in Fig 4a). Correspondingly, the single current path in the chain of particles schematically outlined in Figure 4b consists of several such MNM units connected in series, where the orientation of the xz-plane of the individual units can be different. We conclude that the main contribution to the charge transport in chains of particles is provided by hopping. This mechanism can be regarded as a series of discrete steps initially involving the hopping (injection) of a charge from the left-hand-side electrode to the MNM unit, tunnelling of the charge through the MNM unit, hopping to the next MNM unit, etc., and finally hopping (extraction) of the charge to the right-hand-side electrode. An evaluation of the contact resistance and that of the MNM unit was deduced from the I_0–V curves in Figure 3a (Curve 3) and Figure 3b (Curve 2) with (2), where E_a, $R_m = \alpha_\infty L$, and R_0 were treated as variable parameters. It is found that a good agreement between the experimental data and the model for Sample 1 is obtained with $E_a = 24$ meV, $R_0 = 2.7{\cdot}10^9\ \Omega$, and $R_m = 3.5{\cdot}10^7\ \Omega$. For Sample 2, we had to take $E_a = 25$ meV, $R_0 = 4.4{\cdot}10^{10}\ \Omega$, and $R_m = 1.2{\cdot}10^9\ \Omega$. We, furthermore, deduced that the contact resistance R_0 is larger than R_m by about one order of magnitude for all samples investigated. The resistance R_m means the sum of resistance contributions described with (1) and (2) excluding R_0. It is not possible to separate these two contributions to charge transport on the basis of I–V characteristics. Moreover, the influence of the interface molecule–molecule (most likely via an O–O link) cannot clearly be identified. Hereto, measurements of the I–V curves at different temperatures would be necessary.

Figure 3c and 3d show that the fluctuations of $\mathrm{d}I_0/\mathrm{d}V(V)$ are not exactly periodic. The mean period ΔV of these fluctuations can be roughly evaluated to about 0.5 – 1 mV for Sample 1 and 5 – 7 mV for Sample 2. The ratio of the values of ΔV for different samples correlates with the ratio of the values of the contact resistance R_0. Consequently, we believe that the fluctuations of the differential conductance $\mathrm{d}I_0/\mathrm{d}V(V)$ most likely originate from the Au_e–O interface, as a result of the interplay between molecular conformation, charge switching, and breaking of the links. The quasi-periodicity of the $\mathrm{d}I_0/\mathrm{d}V(V)$ fluctuations can be understood as a consequence of the rotation of the O–C–O group around the C–C axis of the citrate molecule (at the Au_e–O interface). When many citrate molecules connected in parallel participate at the charge transport, only the 'mean frequen-

cies' of $dI_0/dV(V)$ oscillations can be observed experimentally (Fig. 3).

We have demonstrated that, for all samples investigated, the conductance of a sample, deduced from two sequentially measured *I–V* curves, decreases for the third and all following measurements. The latter can be caused due to the displacement of the particles within a chain, caused by the acting electric field or due to the heating of the sample at the interface electrode–molecule as a consequence of the high contact resistance.

5. Conclusion

We have bridged a pair of gold electrodes through small and wide chains of gold nanoparticles, which were stabilized by a coating of citrate molecules. We performed a comparative analysis of current–voltage characteristics for chains of nanoparticles having variable size. Besides stochastic current fluctuations at a constant bias voltage and quasi-periodic fluctuations of the differential conductance arising from conformational changes of citrate molecules, we also observed that the arrangement and distribution of nanoparticles can be changed by the electric field applied, contributing to conductance fluctuations and leading to irreversible changes and finally rupture of the conducting bridge. Although in all cases gold is bridged by the same citrate molecules, a significantly higher resistance between gold electrodes and the citrate coated gold nanoparticles was found as compared to the resistance between identical nanoparticles. Such difference is attributed to the fact that citrate molecules are chemically attached to the nanoparticles, but are only physically interacting with the electrodes. Thus, the resistance of the bridge is not only a function of the number of molecular contacts, but also depends on the strength of the individual interactions between metal conductor and molecules.

Acknowledgement

The authors acknowledge G. Reiter and G.H. Bauer for discussion of the experimental results. This work was financially supported by the Deutsche Forschungsgemeinschaft (DFG) under the grant number PA 378/10-2 and funding by EWE AG Oldenburg.

[1] A. A. Middleton and N. S. Wingreen, Phys. Rev. Lett. **71**, 3198 (1993).
[2] R. Parthasarathy, X. M. Lin, and H. M. Jaeger, Phys. Rev. Lett. **87**, 186807 (2001).
[3] K. Elteto, X. M. Lin, and H. M. Jaeger, Phys. Rev. B **71**, 205412 (2005).
[4] J. Turkevich, P. C. Stevenson, and J. Hillier, Discuss. Faraday Soc. **11**, 55 (1951).
[5] K. Wang, N. L. Rangel, S. Kundu, J. C. Sotelo, R. M. Tovar, J. M. Seminario, and H. Liang, J. Am. Chem. Soc. **131**, 10447 (2009).
[6] L. V. Govor, G. H. Bauer, G. Reiter, and J. Parisi, Phys. Rev. B **82**, 155437 (2010).
[7] L. V. Govor, G. H. Bauer, T. Lüdtke, R. J. Haug, and J. Parisi, Phys. Lett. A **375**, 4041 (2011).
[8] L. V. Govor, G. H. Bauer, T. Lüdtke, R. J. Haug, and J. Parisi, Phys. Status Solidi RRL **6**, 16 (2012).
[9] L. V. Govor, G. H. Bauer, and J. Parisi, Rev. Sci. Instrum. **81**, 106108 (2010).
[10] An aqueous dispersion of gold nanoparticles with a diameter of 20 nm stabilized with citrate (initial concentration $1.2 \cdot 10^{12}$ particles/mL) was purchased from British Biocell International, U.K.
[11] A. Bezryadin, R. M. Westervelt, and M. Tinkham, Appl. Phys. Lett. **74**, 2699 (1999).
[12] K. Elteto, E. G. Antonyan, T. T. Nguyen, and H. M. Jaeger, Phys. Rev. B **71**, 064206 (2005).
[13] H. Ishii, K. Sugiyama, E. Ito, and K. Seki, Adv. Mater. **11**, 605 (1999).
[14] S. Braun, W. R. Salaneck, and M. Fahlman, Adv. Mater. **21**, 1450 (2009).
[15] S. Karthäuser, J. Phys.: Condens. Matter **23**, 013001 (2011).
[16] S. J. van der Molen and P. Liljeroth, J. Phys.: Condens. Matter **22**, 133001 (2010).
[17] J. Kunze, I. Burgess, R. Nichols, C. Buess-Herman, and J. Lipkowski, J. Electroanal. Chem. **599**, 147 (2007).
[18] M. Mabuchi, T. Takenaka, Y. Fujiyoshi, and N. Uyeda, Surface Sci. **119**, 150 (1982).
[19] Z. J. Donhauser, B. A. Mantooth, K. F. Kelly, L. A. Bumm, J. D. Bumm, J. D. Monnell, J. J. Stapleton, D. W. Rice Jr., A. M. Rawlett, D. L. Allara, J. M. Tour, and P. S. Weiss, Science **292**, 2303 (2001).
[20] G. K. Ramachandran, T. J. Hopson, A. M. Rawlett, L. A. Nagahara, A. Primak, and S. M. Lindsay, Science **300**, 1413 (2003).
[21] S. L. Lim, N.-J. Li, J.-M. Lu, Q.-D. Ling, C. X. Zhu, and E.-T. Kang, ACS Appl. Mater. Interfaces **1**, 60 (2009).

[22] J. Repp, G. Meyer, F. E. Olsson, and M. Persson, Science **305**, 493 (2004).
[23] F. E. Olsson, S. Paavilainen, M. Persson, J. Repp, and G. Meyer, Phys. Rev. Lett. **98**, 176803 (2007).
[24] S. W. Wu, N. Ogawa, G. V. Nazin, and W. Ho, J. Phys. Chem. C **112**, 5241 (2008).
[25] S. Floate, M. Hosseini, M. R. Arshadi, D. Ritson, K. L. Young, and R. J. Nichols, J. Electroanal. Chem. **542**, 67 (2003).
[26] F. Tarazona-Vasquez and P. B. Balbuena, J. Phys. Chem. **108**, 15992 (2004).
[27] F. Chen, X. Li, J. Hihath, Z. Huang, and N. Tao, J. Am. Chem. Soc. **128**, 15874 (2006).
[28] R. L. McCreery, Chem. Mater. **16**, 4477 (2004).
[29] L. Luo, S. H. Choi, and C. D. Frisbie, Chem. Mater. **23**, 631 (2011).